Impact of climate change and variability on the global oceanic sink of CO_2

Corinne Le Quéré,[1,2] Taro Takahashi,[3] Erik T. Buitenhuis,[1] Christian Rödenbeck,[4] and Stewart C. Sutherland[3]

Received 5 June 2009; revised 20 January 2010; accepted 24 May 2010; published 26 October 2010.

[1] About one quarter of the CO_2 emitted to the atmosphere by human activities is absorbed annually by the ocean. All the processes that influence the oceanic uptake of CO_2 are controlled by climate. Hence changes in climate (both natural and human-induced) are expected to alter the uptake of CO_2 by the ocean. However, available information that constrains the direction, magnitude, or rapidity of the response of ocean CO_2 to changes in climate is limited. We present an analysis of oceanic CO_2 trends for 1981 to 2007 from data and a model. Our analysis suggests that the global ocean responded to recent changes in climate by outgassing some preindustrial carbon, in part compensating the oceanic uptake of anthropogenic CO_2. Using a model, we estimate that climate change and variability reduced the CO_2 uptake by 12% compared to a simulation where constant climate is imposed, and offset 63% of the trend in response to increasing atmospheric CO_2 alone. The response is caused by changes in wind patterns and ocean warming, with important nonlinear effects that amplify the response of oceanic CO_2 to changes in climate by > 30%.

Citation: Le Quéré, C., T. Takahashi, E. T. Buitenhuis, C. Rödenbeck, and S. C. Sutherland (2010), Impact of climate change and variability on the global oceanic sink of CO_2, *Global Biogeochem. Cycles*, *24*, GB4007, doi:10.1029/2009GB003599.

1. Introduction

[2] Atmospheric CO_2 increased by an average of 1.6 μatm/yr between 1981 and 2007 in response to CO_2 emissions from human activities [*Keeling and Whorf*, 2005]. If no changes in the ocean's physical and biological state had occurred, we would expect the partial pressure of CO_2 at the ocean surface (pCO_2) to have increased also, at a rate that lags slightly behind that of atmospheric CO_2 because of the slow rates for mixing between the surface and deep ocean waters as well as air-sea gas transfer. The difference in rates of increase between the ocean and the atmosphere causes changes in the oceanic CO_2 sink.

[3] Several studies have reported rates of change in the oceanic pCO_2 that are inconsistent with the expected rate. pCO_2 at the most complete existing time series in Bermuda increased at the same rate as atmospheric CO_2 [*Bates*, 2007; *Gruber et al.*, 2002]. Oceanic pCO_2 increased faster than atmospheric CO_2 in the subpolar [*Lefèvre et al.*, 2004; *Corbière et al.*, 2007] and subtropical [*Schuster and Watson*, 2007; *Schuster et al.*, 2009] North Atlantic, subtropical Pacific [*Dore et al.*, 2003; *Keeling et al.*, 2004], South Indian Ocean [*Metzl*, 2009], and in the Southern Ocean winter [*Takahashi et al.*, 2009a]. In contrast, pCO_2 increased generally at the expected rate or slower in the North and South Pacific [*Takahashi et al.*, 2006]. In the equatorial Pacific, large decadal variations were observed [*Feely et al.*, 2006; *Ishii et al.*, 2009]. The observed pCO_2 trends in the Southern Ocean are consistent with trends inferred from atmospheric CO_2 observations [*Le Quéré et al.*, 2007].

[4] A global estimate of changes in the air-sea CO_2 flux is difficult to construct from the synthesis of regional studies because (1) measurements are often fragmented in time and space, (2) the seasonal cycle is not known over large parts of the ocean, and (3) the limited understanding of the sea-air CO_2 transfer rate introduces large errors in the flux estimates. We analyzed observations of surface ocean pCO_2 for the 1981 to 2007 time period using a global database which includes most of the data cited above and other observations compiled by *Takahashi et al.* [2009b] (Version 2008). Our analysis addresses the problems associated with different time periods and maximizes the area of the ocean where pCO_2 trends can be estimated with existing observations [*Takahashi et al.*, 2009a]. We quantified the impact of the trends in sea-air pCO_2 (ΔpCO_2) on the oceanic CO_2 sink using a global general circulation model coupled to an

[1]School of Environmental Sciences, University of East Anglia, Norwich, UK.
[2]British Antarctic Survey, Cambridge, UK.
[3]Lamont-Doherty Earth Observatory of Columbia University, Palisades, New York, USA.
[4]Max Planck Institut für Biogeochemie, Jena, Germany.

0886-6236/10/2009GB003599

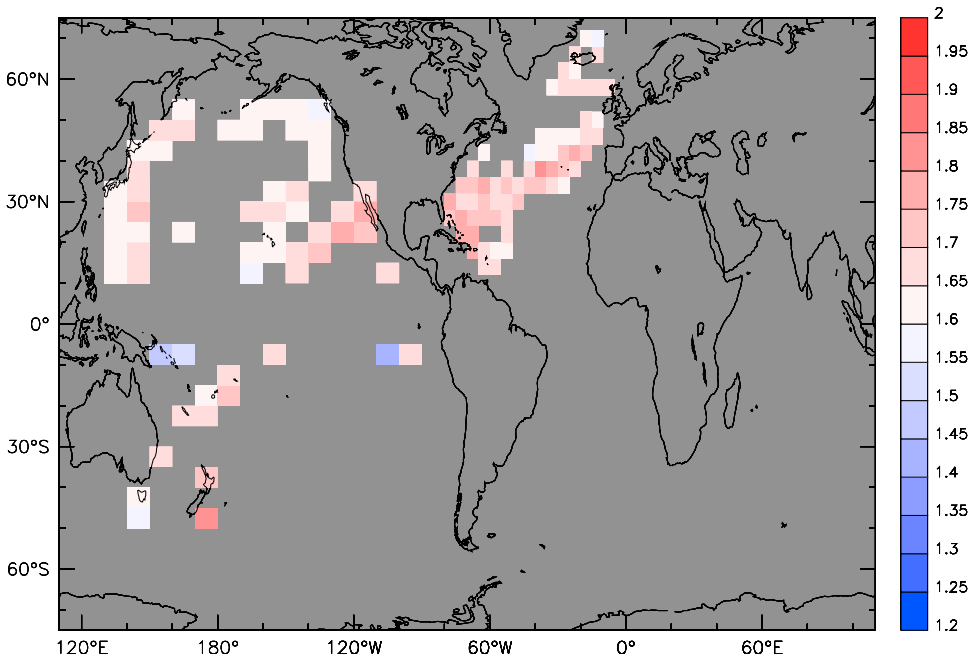

Figure 1. Trend in the atmospheric CO_2 at locations where oceanic pCO_2 trends were computed (ppm/yr). The global mean deseasonalized atmospheric CO_2 was used [*Conway et al.*, 1994] and sampled for each location at months where oceanic pCO_2 observations were available. We assume that there are no trends in the conversion from ppm to μatm and use these estimates directly to calculate ΔpCO_2.

ocean biogeochemistry model and forced by meteorological data.

2. Methods

2.1. Data Analysis

[5] Using the about 3 million pCO_2 observations in the database, decadal trends in surface water pCO_2 for 27% of the global ocean areas can be determined. The decadal pCO_2 trends were computed in boxes of 4° × 5° (North Atlantic) or 5° × 10° (Pacific) where (1) the seasonal cycle of pCO_2 could be clearly defined with observations made in at least three consecutive years, (2) observations were distributed evenly over the three decades, and (3) the first year observed was 1985 or before (see Text S1).[1] The decadal trends were computed using a linear regression to the monthly mean values for deseasonalized data as described by *Takahashi et al.* [2006, 2009a]. The method was tested using the SST data concurrent with the pCO_2 observations, and ensuring that trends estimated with concurrent SST data were consistent with SST trends derived from continuous measurements [*Shea et al.*, 1992].

[6] The uncertainty in the mean time-trend was computed by:

$$\pm[\sigma^2/(\Sigma(X_i^2) - N(X_{mean})^2)]^{1/2},$$

where $\sigma^2 = [(\Sigma(Yi - aX_i - b)^2)/(N\text{-}2)]$ is the variance around the fitted equation $Y = a\,X + b$, and Y is pCO_2 or SST and X is year.

[7] The mean pCO_2 trend for the Southern Ocean (south of 50°S) was computed for six circumpolar zones defined by SST intervals of ~1°C between 0.80°C and 6.50°C, using only data between year days 172 through 326, without deseasonalization. This period represents winter conditions extending into spring but prior to the onset of intense pCO_2 drawdown due to phytoplankton blooms. The six zones were averaged. The first year observed varied from 1981 to 1991 in the different regions (see Text S1).

[8] Since the atmospheric CO_2 rise accelerated during our study period, the trend depends on the time period. To be consistent with our analysis of pCO_2 trends in the ocean, we estimated the trends in atmospheric CO_2 by sampling the observed global mean trend for each ocean box at the month where oceanic observations were available. We used the global mean deseasonalized atmospheric CO_2 concentration (updated from *Conway et al.* [1994]) because the ship air CO_2 measurements were not everywhere available. The impact on pCO_2 of time trends in atmospheric pressure is very small (<0.001 μatm/yr) and neglected in this analysis, and hence the ppm/yr may be equated with μatm/yr. The trend in atmospheric CO_2 using all the data is 1.61 ppm/yr (or μatm/yr). When the data is sampled like the oceanic observations, the trend averages to 1.68 ± 0.07 (mean ± one standard deviation; see Figure 1). The trend was 1.62 and 1.60 in the western warm pool and Southern Ocean, respectively. We computed the error on the atmospheric CO_2 trend

[1] Auxiliary materials are available with the HTML. doi:10.1029/2009GB003599.

Table 1. Contribution of Atmospheric CO_2 and Climate to Mean Decadal Trends in Sea-Air CO_2 Flux (PgC/yr per decade)[a]

	Atmospheric Inversion[b]	Ocean Model						
				Climate Only[c]				
Region	CO_2 and Climate[b]	CO_2 and Climate[c]	CO_2 Only[c]	All	Temperature	Wind	Heat and Water Fluxes	Nonlinear Effects
Globe	0.17 ± 0.12	−0.12	−0.32	0.20	0.04	0.12	−0.03	0.06
30°N–90°N	−0.03 ± 0.02	−0.05	−0.05	0.01	0.03	0.00	−0.03	0.01
30°S–30°N	0.18 ± 0.09	−0.01	−0.14	0.13	0.01	0.08	−0.01	0.04
90°S–30°S	0.01 ± 0.03	−0.06	−0.13	0.06	0.01	0.04	0.00	0.01

[a]Trends are calculated over the 1981–2007 time period unless indicated otherwise. Negative values indicate an enhanced flux from the atmosphere to the ocean (increasing sink).
[b]1981–2004 only. Median ± 1 mean absolute deviation around the median, for the ten inversions presented by *Le Quéré et al.* [2007], excluding the two sensitivity tests where the winds were kept constants.
[c]See section 2.2 for description of terms.

using the same method as for oceanic pCO_2 trend. We used the local estimate of atmospheric CO_2 trends and its associated error (Figure 1) to calculate the ΔpCO_2.

[9] The analysis presented here is similar to that presented by *Takahashi et al.* [2009a], but the time period selected (1981–2007) is more homogeneous across regions, we estimated trends in ΔpCO_2 rather than oceanic pCO_2 alone, and we included additional data submitted recently to the global surface pCO_2 database of *Takahashi et al.* [2009b]. The ~1,100 additional data used in this study (added to 66,240 observations used to compute trends by *Takahashi et al.* [2009a]) cover mainly year 2007. The data analysis presented here is identical to that used by *Le Quéré et al.* [2009, Figure 3]. It is shown here using a more detailed scale and does not include the additional South Indian Ocean trends from *Metzl* [2009], which cover a different time period.

2.2. Model Simulations

[10] We used an Ocean General Circulation Model [*Madec and Imbard*, 1996] with horizontal resolution of ~1.5 × 2 degree, 30 vertical levels, explicit vertical diffusion and parameterized eddy mixing [*Le Quéré et al.*, 2007]. The model is coupled to a marine biogeochemistry model [*Buitenhuis et al.*, 2006] with no nutrient restoring. It is forced by increasing atmospheric CO_2 data [*Keeling and Whorf*, 2005] and daily winds and precipitation from NCEP reanalysis [*Kalnay et al.*, 1996]. The model calculates sensible and latent heat fluxes from the temperature difference between the modeled surface temperature and the observed air temperature using a bulk formulation. Simulations are initialized from observations using temperature, salinity and nutrients from the World Ocean Atlas 2005 [*Locarnini et al.*, 2006; *Antonov et al.*, 2006; *Garcia et al.*, 2006], and the total CO_2 concentration in seawater and alkalinity fields in seawater from *Key et al.* [2004]. Total CO_2 concentration was corrected to the initial year of the simulation using the estimate of *Sabine et al.* [2004] scaled to the increase in atmospheric CO_2 from the corresponding time period. Other fields were initialized with results from previous simulations.

[11] The individual contributions of temperature, winds, fluxes and atmospheric CO_2 presented in Tables 1 and 2 were computed by turning off individual forcing or processes in a series of six simulations (S) as follows:

$$S_1 = d$$

$$S_2 = d + F_A$$

$$S_3 = d + F_A + F_T + F_W + F_F$$

$$S_4 = d + F_A + F_F + F_W$$

$$S_5 = d + F_A + F_F$$

$$S_6 = d + F_A + F_W$$

where d is the model drift. F_A, F_T, F_W and F_F are the contributions of atmospheric CO_2, temperature effect on CO_2 solubility, winds, and heat and water fluxes, respectively.

Table 2. Contribution of Atmospheric CO_2 and Climate to Mean Decadal Trends in Sea-Air CO_2 Flux (PgC/yr per decade) by Basin[a]

			Climate Only[b]				
Region	CO_2 and Climate[b]	CO_2 Only[b]	All	Temperature	Wind	Heat and Water Fluxes	Nonlinear Effects
30°N–90°N							
Pacific	0.00	−0.02	0.03	0.01	0.01	0.00	0.01
Atlantic	−0.05	−0.03	−0.02	0.02	−0.01	−0.03	0.00
30°S–30°N							
Pacific	0.04	−0.09	0.13	0.00	0.10	0.00	0.03
Atlantic	−0.02	−0.03	0.00	0.01	−0.01	0.00	0.01
Indian	−0.04	−0.03	−0.01	0.00	−0.01	0.00	0.01

[a]Trends are calculated over the 1981–2007 time period unless indicated otherwise. Negative values indicate an enhanced flux from the atmosphere to the ocean (increasing sink).
[b]See section 2.2 for description of terms.

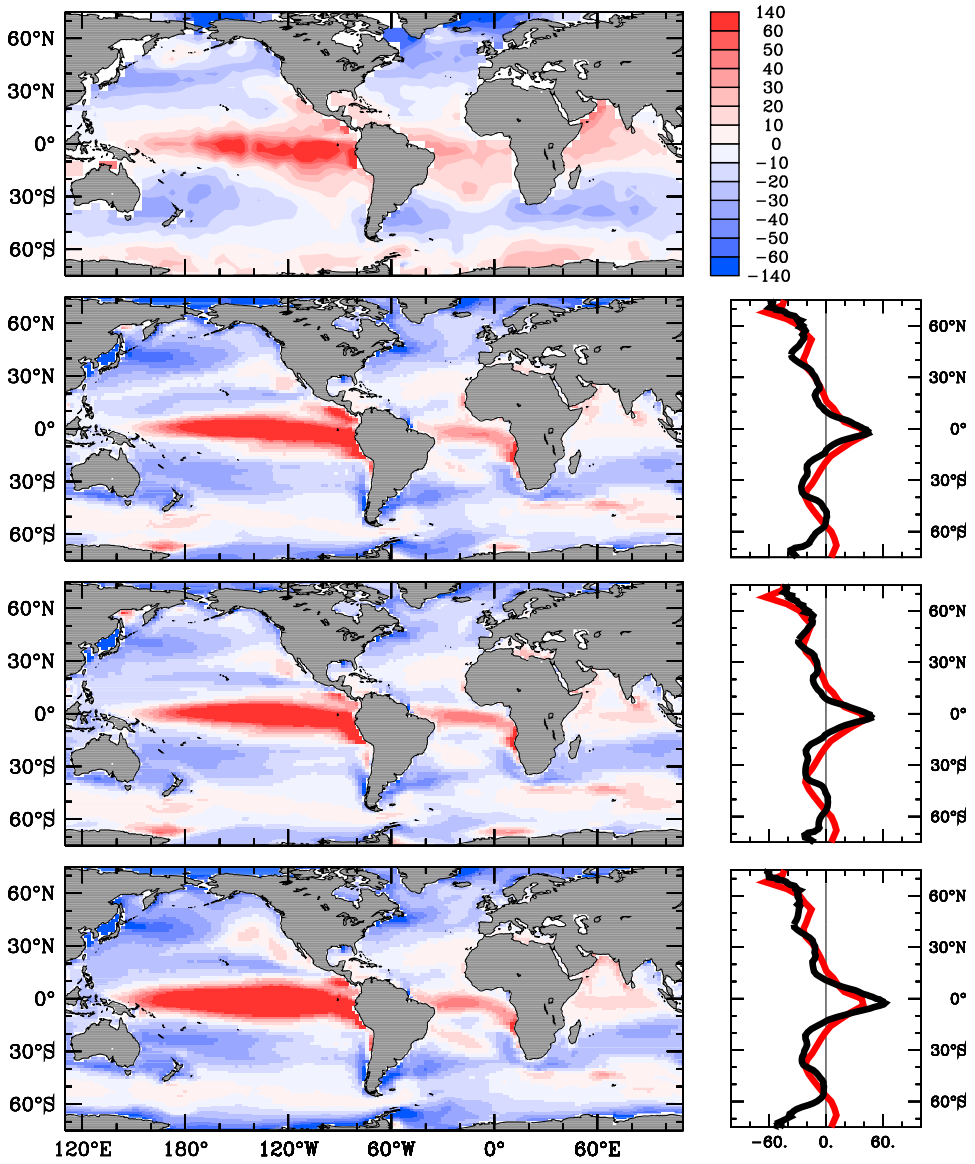

Figure 2. Climatological mean ΔpCO_2 (μatm) from (top plot) observations [*Takahashi et al.*, 2009a], (second plot) the model forced by NCEP reanalysis fields [*Kalnay et al.*, 1996], (third plot) the model forced by NCEP-2 reanalysis [*Kanamitsu et al.*, 2002], and (bottom plot) the model forced by satellite winds [*Atlas et al.*, 1996, 2009]. The right panels show the zonal mean ΔpCO_2 (μatm) for the model (black) and observations (red). The climatology is corrected to year 2000. Model results are averaged between 1995 and 2005.

[12] S_1 is forced by an atmospheric CO_2 of 310 ppm, corresponding to the observed concentration in 1948. The forcing fields loop over the daily fields for year 1967, and thus include no trends or variability in climate. A further small correction is made to take into account the increase in CO_2 that occurred prior to 1948 by using a pulse response model [*Enting et al.*, 1994].

[13] S_2 is forced by the global observed monthly mean atmospheric CO_2, with the forcing fields of year 1967 as in S_1.

[14] S_3 is forced by the global observed monthly mean atmospheric CO_2 and by the daily forcing fields corresponding to the year of the simulation. Thus trends and variability in climate are taken into account.

[15] S_4 is like S_3, except that the model code has been modified to remove the effect of warming on the carbon cycle. To do this, all carbon cycle processes have been calculated with the climatological monthly mean temperature instead of the modeled temperature.

[16] S_5 uses the same model code as S_4 (with no temperature effect). It is forced by the global observed monthly mean atmospheric CO_2 and by the daily forcing fields corresponding to the year of the simulation for the fluxes, but the wind fields loop over the daily fields for year 1967.

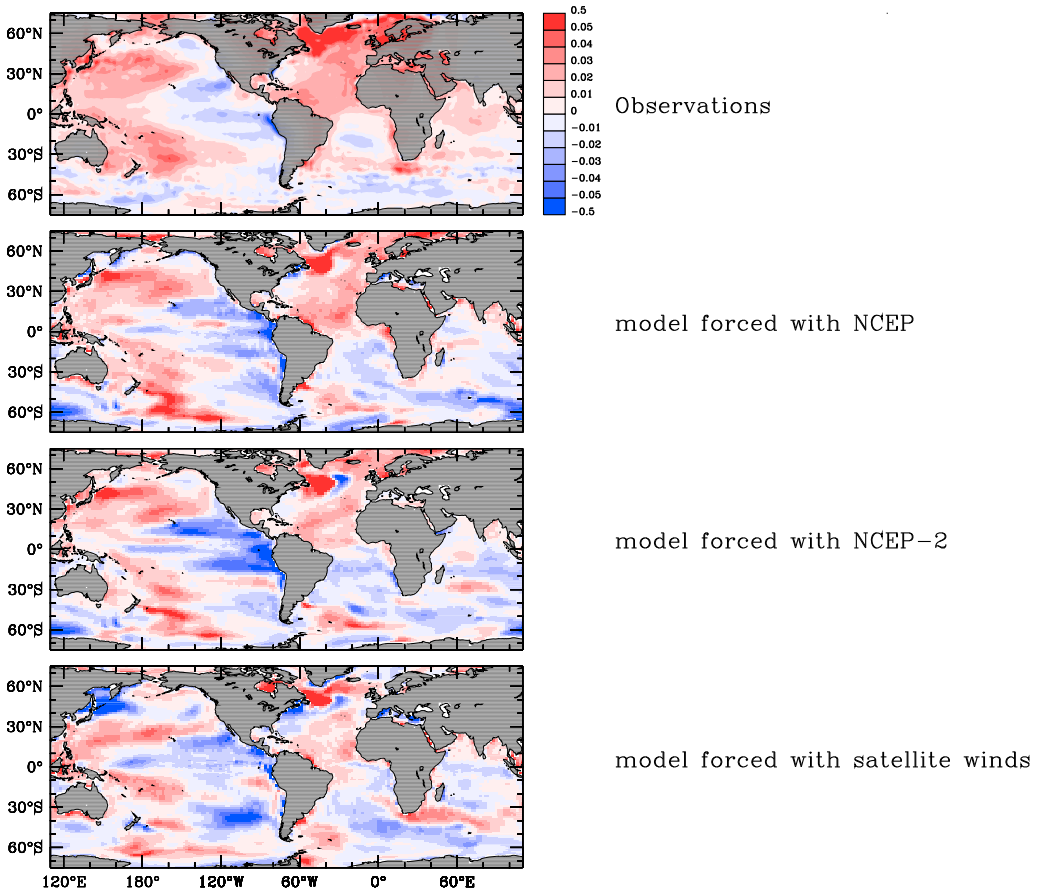

Figure 3. Trend in SST between 1982 and 2007 (°C/yr) from (top plot) observations [*Reynolds et al.*, 2002], (second plot) the model forced by NCEP reanalysis fields [*Kalnay et al.*, 1996], (third plot) the model forced by NCEP-2 reanalysis [*Kanamitsu et al.*, 2002], and (bottom plot) the model forced by satellite winds (1988–2007 only) [*Atlas et al.*, 1996, 2009].

[17] S_6 is as S_5, but with varying winds and fixed flux fields.

[18] The above simulations, when the model is forced by data from NCEP-1 reanalysis, are identical to those used to identify the processes driving the recent weakening of the Southern Ocean CO_2 sink by *Le Quéré et al.* [2007]. These simulations are analyzed here for the global ocean, and other sources of forcing data are used.

[19] In Tables 1 and 2, the contribution of individual processes is computed using the following simulations:

CO_2 and Climate: $S_3 - S_1$

CO_2 only: $S_2 - S_1$

All processes combined: $S_3 - S_2$

Temperature only: $S_3 - S_4$

Wind only: $S_4 - S_5$

Fluxes only: $S_4 - S_6$

[20] In addition to the NCEP-1 forced standard model runs, we explored the impact of atmospheric forcing on the model trends by using atmospheric fields from the NCEP reanalysis-2 estimates [*Kanamitsu et al.*, 2002] and from satellite wind data developed at the Jet Propulsion laboratory [*Atlas et al.*, 1996, 2009]. The latter simulation used fluxes from NCEP-1 reanalysis to complement the satellite-derived wind-forcing. These runs are initialized from the result of the standard simulation in 1970 (for NCEP-2) and in 1978 (for satellite winds). The simulations were run for 10 years using increasing atmospheric CO_2 but constant forcing from year 1980 (for NCEP-2) and 1990 (for JPL). These are the earliest years in the forcing products which do not have El Niño events or other large scale interannual anomalies. Subsequent years were forced by daily fields from the corresponding year and product. All three model simulations reproduce the broad patterns of the annual mean ΔpCO_2 and the trends in sea surface temperature present in the observations (Figures 2 and 3).

[21] We also repeated run S2 (constant daily mean forcing fields with increasing atmospheric CO_2), but repla-

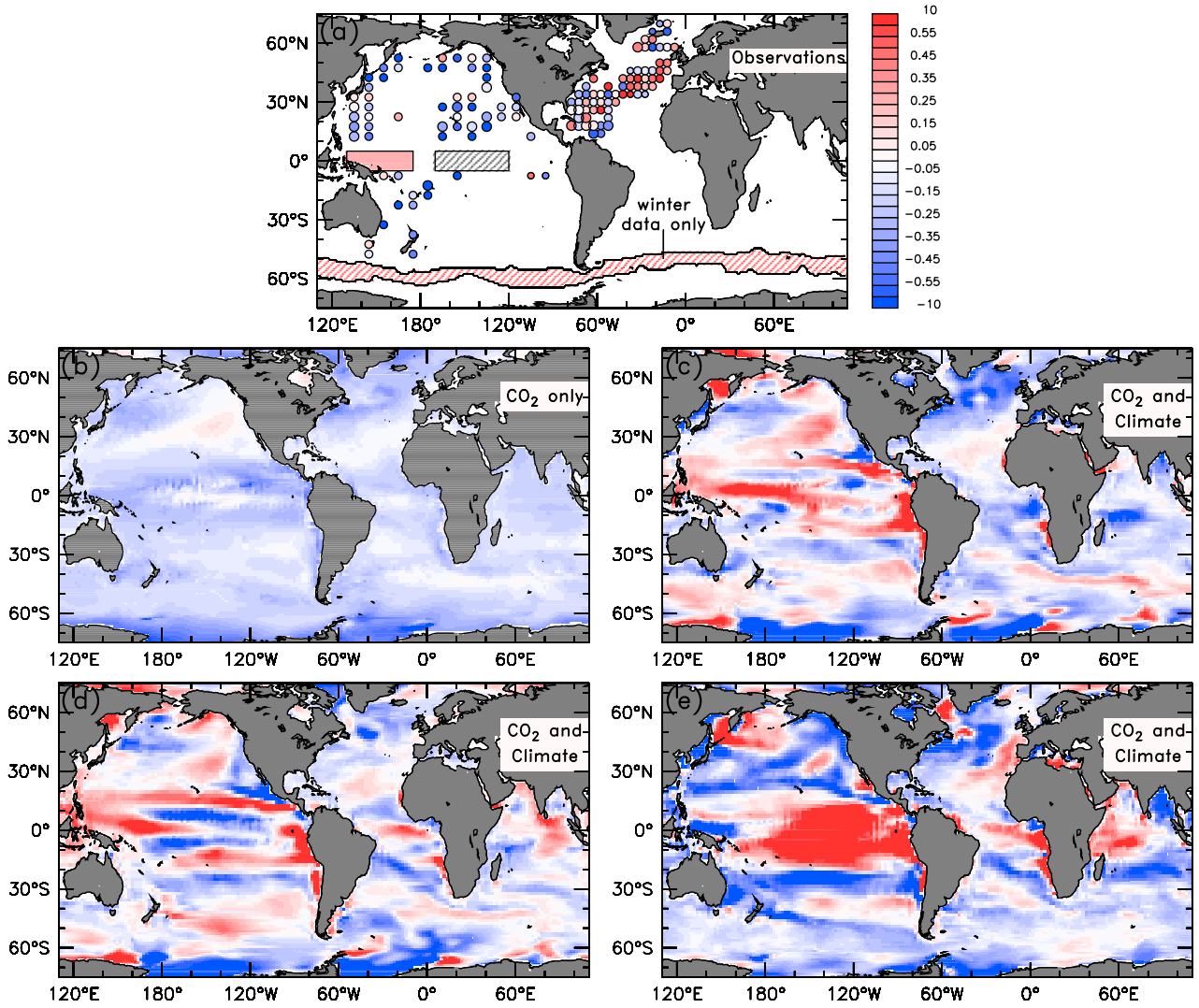

Figure 4. Trend in ΔpCO_2 (μatm/yr) between 1981 and 2007. (a) From observations. Large, medium and small dots are plotted for trends with errors < 0.25, 0.25 to 0.50, and > 0.50 μatm/yr, respectively. A single trend is shown for the Southern Ocean representing the circumpolar averaged for temperature between 0.8 and 6.5°C and winter observations only (see section 2). The gray box in the central equatorial Pacific identifies the El Niño 3.4 region where observations exist but the variability is too large to identify a trend. See section 2 for details of calculation. (b) From a model forced by increasing atmospheric CO_2 alone. (c to e) From a model forced by both increasing atmospheric CO_2 and changes in climate as provided by the NCEP reanalysis [*Kalnay et al.*, 1996] (Figure 4c), NCEP-2 reanalysis [*Kanamitsu et al.*, 2002] (Figure 4d), and a satellite wind product [*Atlas et al.*, 1996, 2009] with NCEP fluxes (1988–2007 only; Figure 4e). White values represent regions where the oceanic pCO_2 trend is following atmospheric CO_2. Blue values are regions where the oceanic trend is slower than atmospheric CO_2 (expected signal). Red values are regions where oceanic pCO_2 is increasing faster than atmospheric CO_2, indicating regions where natural CO_2 is outgassed to the atmosphere compared to the pre-1981 state.

cing the forcing fields from year 1967 by those from year 1948.

3. Results

[22] The difference between the pCO_2 in seawater and in the atmosphere (ΔpCO_2) shows coherent changes in large parts of the world's oceans (Figure 4a). Oceanic pCO_2 increased faster than atmospheric CO_2 in the North Atlantic (positive rate of change in ΔpCO_2), western tropical Pacific, and Southern Ocean (winter only), and slower than atmospheric CO_2 (negative rate of change in ΔpCO_2) in the North and South Pacific, consistent with regional analysis [*Schuster et al.*, 2009; *Takahashi et al.*, 2006, 2009a].

Table 3. Contribution of Climate to Mean Decadal Trends in Sea-Air CO_2 Flux (PgC/yr per decade) in Different Ocean Model Simulations[a]

Region	Climate Only NCEP Forcing Compared to Constant Forcing for Year 1967	Climate Only NCEP Forcing Compared to Constant Forcing for Year 1948	Climate Only NCEP-2 Forcing Compared to Constant Forcing for Year 1980	Climate Only JPL Winds Compared to Constant Forcing for Year 1990
Globe	0.20	0.16	0.21	0.15[b]
30°N–90°N	0.01	0.01	0.00	0.01[b]
30°S–30°N	0.13	0.11	0.15	0.17[b]
90°S–30°S	0.06	0.04	0.06	−0.02[b]

[a]The first column is repeated from Table 1. The second column uses NCEP forcing for year 1948 (instead of 1967) when no climate change is imposed. The two right columns are computed with forcing from NCEP-2 and JPL satellite data. Trends are calculated over the 1981–2007 time period for simulations forced with NCEP and NCEP-2, and over 1988–2007 for the simulation forced with satellite winds. Negative values indicate an enhanced flux from the atmosphere to the ocean (increasing sink).
[b]Trends calculated over 1988–2007 only.

[23] When the model is forced by increasing atmospheric CO_2 alone (no changes in climate), the ΔpCO_2 decreases as expected (Figure 4b), but the regional patterns of ΔpCO_2 in this simulation are very different from the observations (Figures 4a and 4b). When the model is forced by both the increasing atmospheric CO_2 and by changes in climate, the trends in ΔpCO_2 show strong regional patterns (Figure 4c). In the Southern Ocean, the model produces no change in ΔpCO_2 indicating nearly no change in the CO_2 sink, compared to a ΔpCO_2 of about −0.1 μatm/yr when the model is forced by increasing CO_2 alone (no changes in climate). When the model is sampled at the same location and month as the observations and averaged by temperature bands (see section 2), the trend in modeled ΔpCO_2 increases to 0.4 μatm/yr, close to the observed trend of 0.5 ± 0.6 μatm/yr, and clearly above the trend of −0.2 μatm/yr for the sampled model forced by increasing CO_2 alone. *Metzl* [2009] observed similar trends in ΔpCO_2 for 1991–2007 for all seasons in the South Indian ocean.

[24] In the western equatorial Pacific, the model produces an increase in ΔpCO_2 of 0.4 μatm/yr, close to the observed trend of 0.3 ± 0.2 μatm/yr, and clearly above the trend of −0.2 μatm/yr for the model forced by increasing CO_2 alone. In the El Niño 3.4 region however, it is not possible to calculate a trend from observations because of the preeminent interannual variability associated with the El Niño Southern Oscillation (ENSO). However, the modeled pCO_2 correlates to the observations with r = 0.93, showing that it captures most of the observed variability.

[25] The model produces a negative trend in ΔpCO_2 in the western South Pacific, as observed. It also produces large regional variability in the North Pacific, although the regional patterns do not match the observations everywhere. Finally, the model underestimates the large positive ΔpCO_2 trends in the North Atlantic and locates its position further to the South. The regional patterns in ΔpCO_2 forced with NCEP-2 [*Kanamitsu et al.*, 2002] and the JPL satellite data [*Atlas et al.*, 1996, 2009] also show large spatial variability in ΔpCO_2, but the location and amplitude of the regional patterns are sensitive to the atmospheric forcing (Figures 4c to 4e).

[26] We used the model to estimate the corresponding trends in sea-air CO_2 fluxes. When the model is forced by increasing atmospheric CO_2 alone (no changes in climate), the global oceanic CO_2 sink increases at a 1981–2007 mean

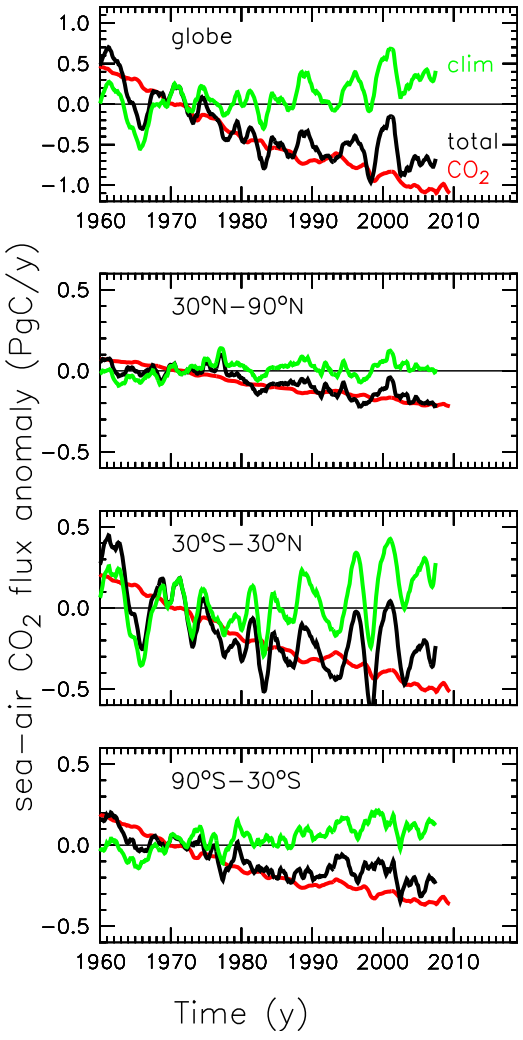

Figure 5. Modeled anomaly in sea-air CO_2 flux (PgC/yr). Results are shown for (top plot) the global ocean and (second, third, and bottom plots) by latitude bands. The contribution of atmospheric CO_2 alone (red), climate change and climate variability (green) and the sum of the two (black) are shown for each plot. Anomalies are computed with respect to 1960–1981 time period.

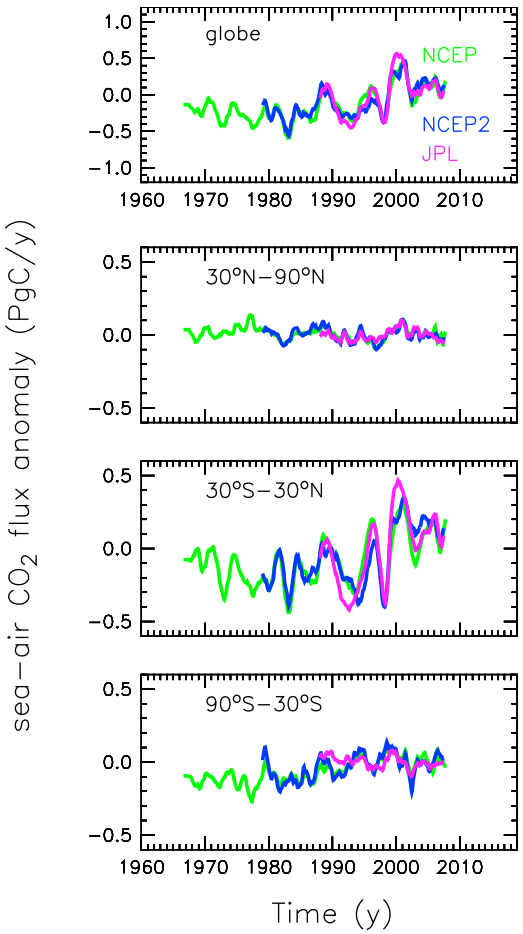

Figure 6. Climate impact on the sea-air CO_2 flux in simulations using NCEP forcing [*Kalnay et al.*, 1996] (green, identical to Figure 5), NCEP-2 forcing [*Kanamitsu et al*, 2002] (blue), and satellite winds [*Atlas et al.*, 1996, 2009] (purple).

rate of 0.32 PgC/yr per decade (Table 1 and Figure 4). However, when the model is forced by both increasing atmospheric CO_2 and by changes in climate, this rate is only 0.12 PgC/yr per decade. Thus the effect of changes in climate is to reduce the rate of increase of the global oceanic CO_2 sink by 0.20 PgC/yr per decade. The reduction due to the climate response is largest in the equatorial Pacific (0.13 PgC/yr per decade) and Southern hemisphere (0.06 PgC/yr per decade). These results are generally consistent across the range of forcing used, with the global reduction due to climate ranging between 0.15 and 0.21 and the dominance of the tropical signal (Table 3 and Figure 5). The simulation forced by satellite data does not produce a weakening of the Southern Ocean CO_2 sink as the other two simulations because it starts later (in 1988) and the first five years of the simulations show a higher sea-air CO_2 flux (Figure 5).

4. Discussion

[27] Changes in trends occur on top of a global CO_2 sink that averages to 2.2 PgC/yr for the 1990s [*Denman et al.*, 2007]. Over the 1981–2007 time period (27 years), if the global oceanic sink had not changed, the oceanic uptake would have been 59.4 PgC. This is very close to the CO_2 uptake estimated with the model forced by increasing atmospheric CO_2 and climate change and variability (60.4 PgC). The trend caused by the increase in atmospheric CO_2 alone should cause the global sink to increase at a rate of 0.32 PgC/yr per decade, which amounts to an additional uptake of 11.7 PgC (+20%). We estimated that the trend caused by climate change and variability decreased the global sink at a rate of 0.20 PgC/yr per decade, which amounts to a loss of 7.3 PgC (−12%). Thus changes in climate compensated ~63% of the increase in CO_2 sink that is attributable to atmospheric CO_2 alone.

[28] To isolate the contributions of changes in different components of atmospheric forcing we performed a series of model experiments (section 2). Our experiments show that 20% of the impact of changes in atmospheric climatic conditions can be explained directly by the response of surface ocean pCO_2 to surface warming (Table 1). The relative contribution of warming on the CO_2 flux trend can be estimated directly from the observations. In the North Pacific, the mean rate of increase in observed pCO_2 was +13.1 ± 0.5 μatm per decade for a SST trend of +0.2 ± 0.05°C per decade (section 2). Using a temperature effect of 4.23% pCO_2/°C and 350 μatm for the mean pCO_2 gives a temperature contribution to pCO_2 of 3.0 μatm per decade, or 23% of the total signal. A similar calculation for the North Atlantic data yields a temperature contribution of 25%.

[29] Changes in oceanic circulation due to changes in winds caused the largest effect (Table 1). The wind changes were particularly important in the equatorial Pacific where enhanced upwelling caused more CO_2 to outgas, and in the Southern Ocean (Figure 5). The impact of wind changes on the gas exchange formulation are small [*Le Quéré et al.*, 2007] and nearly all the impact of wind changes in the model simulations was caused by changes in ocean circulation. Changes in the heat and water fluxes were only important in the Northern hemisphere. The sum of the individual components accounted for 65% of the total effect only. The remainder is caused by nonlinear effects. Nonlinear effects are maximum in the tropics, where upwelling combined with surface warming lead to additional outgassing of CO_2.

[30] The choice of forcing fields is important to determine regional trends and could account for some of the data-model mismatch (Figure 6). In particular, the North Atlantic is more sensitive to heat and water fluxes than other regions. Heat and water fluxes are difficult to estimate and vary widely across reanalysis products. Our sensitivity study suggests that regional and global CO_2 trends are very sensitive to trends in atmospheric conditions, particularly winds but also heat and water fluxes, and that more attention need to be given to projections of trends in these variables in a changing climate in order to improve projections of the oceanic CO_2 sink in the future.

[31] Our model results are consistent with three sets of observations. First the modeled trends in SST are consistent with observations [*Reynolds et al.*, 2002]. Second, the modeled trends in ΔpCO_2 agree with available observations in the Southern Hemisphere and equatorial Pacific,

where the model shows the largest climatic impacts. Finally, we compared the trends in CO_2 fluxes estimated by our model with estimates from a series of atmospheric CO_2 inversions [*Le Quéré et al.*, 2007] (Table 1). Atmospheric inversions use measurements of atmospheric CO_2 distributed around the world to estimate CO_2 fluxes at the earth's surface. This method provides weak constraints only because of the influence of the large land CO_2 fluxes in the Northern hemisphere and tropics, and because of potential issues with early data. Nevertheless, the trends estimated from the atmospheric data are even more positive than those simulated by our ocean model forced by increasing atmospheric CO_2 and changes in climate. Despite the large uncertainties, this would suggest that results from the model forced by atmospheric CO_2 alone are less likely to be a correct representation of reality.

5. Conclusion

[32] Our model analysis suggests that the total effect of climate change and variability between 1981 and 2007 was to weaken the global oceanic CO_2 sink by 0.20 PgC/yr per decade. The changes associated with warming (20%) occurred throughout the oceans and are very likely induced by human activities [*IPCC*, 2007]. The changes associated with increasing winds in the Southern Ocean (20%) have been attributed to human-induced climate change in response to both the depletion of stratospheric ozone [*Thompson and Solomon*, 2002] and to global warming [*Fyfe et al.*, 1999] and are consistent with other model results [*Wetzel et al.*, 2005; *Lovenduski et al.*, 2008]. Although an increase in the upwelling as a cause for the weakening CO_2 sink flux in the Southern Ocean is disputed [*Böning et al.*, 2008], both atmospheric and oceanic observations are consistent with the weakening of CO_2 sink flux in this region. The changes associated with wind changes in the equatorial Pacific (Figure 4) are consistent with decadal variability induced by the Pacific Decadal Oscillation and ENSO variability [*Feely et al.*, 2006]. The nonlinear combination of changes in winds and temperature suggests an enhancement of the natural variability on CO_2 outgassing in the tropics.

[33] Atmospheric CO_2 observations suggest that a weakening of the CO_2 uptake rate by the land and ocean CO_2 reservoirs has occurred since 1958 [*Canadell et al.*, 2007] at a rate of 0.07 ± 0.06 PgC/yr per decade (0.25 ± 0.21%/yr). However, the uncertainty in this estimate is very large. Our analysis suggests that the observed atmospheric signal since 1981 can be accounted for by warming and wind changes occurring over the ocean, consistent with results from land models [*Sitch et al.*, 2008].

[34] **Acknowledgments.** We thank all people who contributed to the pCO_2 database, in particular the following people who contributed the longest time series data used in our study: D. C. E. Bakker, D. W. Chipman, C. E. Cosca, B. Hales, R. Feely, M. Ishii, T. Johannessen, A. Körtzinger, N. Metzl, T. Modorikawa, Y. Nojiri, J. Olafsson, A. Olsen, U. Schuster, C. Sweeney, B. Tilbrook, R. Wanninkhof, A.J. Watson, C. S. Wong. and H. Yoshikawa-Inoue. We thank N. Lefèvre, N. Metzl, B. Tilbrook, N. Gruber and the participants of the IOCCP/GCP workshop for discussions, M.C. Enright and S. Jones for programming support and the OPA team for availability of their model. NCEP reanalysis data was provided by NOAA/OAR/ESRL. We thank J. Ardizzone and the JPL-PODAAC for providing the satellite wind data, and P. Tans and T. Conway of NOAA/ESRL for providing atmospheric CO_2 data. C.L.Q. and E.T.B. were funded by NERC/QUEST and EU Carbo-ocean project (511176/GOCE). T.T. and S.C.S. were supported by a grant from the U.S. NOAA VOS program.

References

Antonov, J. I., R. A. Locarnini, T. P. Boyer, A. V. Mishonov, and H. E. Garcia (2006), *World Ocean Atlas 2005*, vol. 2, *Salinity. NOAA Atlas NESDIS 62*, edited by S. Levitus, 182 pp., U.S. Gov. Print. Off., Washington, D. C.

Atlas, R., R. N. Hoffman, S. C. Bloom, J. C. Jusem, and J. Ardizzone (1996), A Multiyear global surface wind velocity data set using SSM/I wind observations, *Bull. Am. Meteorol. Soc.*, *77*, 869–882, doi:10.1175/1520-0477(1996)077<0869:AMGSWV>2.0.CO;2.

Atlas, R., R. N. Hoffman, J. Ardizzone, S. M. Leidner, and J. C. Jusem (2009), A new cross-calibrated, multi-satellite ocean surface wind product, in *Geoscience and Remote Sensing Symposium, 2008. IGARSS 2008*, pp. 106–109, IEEE Int., New York, doi:10.1109/IGARSS.2008.4778804.

Bates, N. R. (2007), Interannual variability of the oceanic CO_2 sink on the subtropical gyre of the North Atlantic Ocean over the last 2 decades, *J. Geophys. Res.*, *112*, C09013, doi:10.1029/2006JC003759.

Böning, K., A. Dispert, M. Visbeck, S. R. Rintoul, and F. U. Schwarzkopf (2008), The response of the Antarctic Circumpolar Current to recent climate change, *Nat. Geosci.*, *1*, 864–869, doi:10.1038/ngeo362.

Buitenhuis, E., et al. (2006), Biogeochemical fluxes through mesozooplankton, *Global Biogeochem. Cycles*, *20*, GB2003, doi:10.1029/2005GB002511.

Canadell, J. G., et al. (2007), Contributions to accelerating atmospheric CO_2 growth from economic activity, carbon intensity, and efficiency of natural sinks, *Proc. Nat. Acad. Sci.*, *104*, pp. 18,866–18,870, doi:10.1073pnas.0702737104.

Conway, T., P. Tans, L. Waterman, K. Thoning, D. Kitzis, K. Masarie, and N. Zhang (1994), Evidence for interannual variability of the carbon cycle from the national oceanic and atmospheric administration climate monitoring and diagnostics laboratory global air sampling network, *J. Geophys. Res.*, *99*, 22,831–22,855, doi:10.1029/94JD01951.

Corbière, A., N. Metzl, G. Reverdin, C. Brunet, and T. Takahashi (2007), Interannual and decadal variability of the oceanic carbon sink in the North Atlantic subpolar gyre, *Tellus, Ser. B*, *59*(2), 168–178, doi:10.1111/j.1600-0889.2006.00232.x.

Denman, K., et al. (2007), Couplings between changes and biogeochemistry, in *Climate Change 2007: The Physical Science Basis. Contribution of Working Group Report of the Intergovernmental Panel on Climate Change*, edited by S. Solomon et al., pp. 499–588, Cambridge Univ. Press, Cambridge, U. K.

Dore, J. E., R. Lukas, D. W. Sadler, and D. M. Karl (2003), Climate-driven changes to the atmospheric CO_2 sink in the subtropical North Pacific Ocean, *Nature*, *424*, 754–757, doi:10.1038/nature01885.

Enting, I. G., T. M. L. Wigley, M. Heimann (1994), Future emissions and concentrations of carbon dioxide: Key ocean/atmosphere/land analyses, *CSIRO Aust. Div. Atmos. Res. Tech. Pap. 31*, 120 pp.

Feely, R. A., et al. (2006), Decadal variability of the air-sea CO_2 fluxes in the equatorial Pacific Ocean, *J. Geophys. Res.*, *111*, C08S90, doi:10.1029/2005JC003129.

Fyfe, J., G. Boer, and G. Flato (1999), The Arctic and Antarctic Oscillation and their projected changes under global warming, *Geophys. Res. Lett.*, *26*, 1601–1604, doi:10.1029/1999GL900317.

Garcia, H. E., R. A. Locarnini, T. P. Boyer, and J. I. Antonov (2006), *World Ocean Atlas 2005*, vol. 3, *Dissolved Oxygen, Apparent Oxygen Utilization, and Oxygen Saturation*, *NOAA Atlas NESDIS 63*, edited by S. Levitus, 342 pp., U.S. Gov. Print. Off., Washington, D. C.

Gruber, N., C. D. Keeling, and N. R. Bates (2002), Interannual variability in the North Atlantic Ocean carbon sink, *Science*, *298*, 2374–2378, doi:10.1126/science.1077077.

IPCC (2007), Summary for Policymakers (SPM), in *Climate Change 2007: The Physical Science Basis: Contribution of Working Group I to the Fourth Assessment Report of the Intergovernmental Panel on Climate Change*, edited by S. Solomon et al., pp. 1–18, Cambridge Univ. Press, U. K.

Ishii, M., et al. (2009), Spatial variability and decadal trend of the oceanic CO_2 in the western equatorial Pacific warm/fresh water, *Deep Sea Res., Part II*, *56*(8–10), 591–606.

Kalnay, E., et al. (1996), The NCEP/NCAR 40-Year Reanalysis Project, *Bull. Am. Meteorol. Soc. 77*, 437–471.

Kanamitsu, M., et al. (2002), NCEP-DEO AMIP-II Reanalysis (R-2), *Bull. Am. Meteorol. Soc.*, *83*, 1631–1643.

Keeling, C. D., and T. P. Whorf (2005), *Trends: A Compendium of Data on Global Change*, Carbon Dioxide Inf. Anal. Cent., Oak Ridge Natl. Lab., U.S. Dept. of Energy, Oak Ridge, Tenn.

Keeling, C. D., H. Brix, and N. Gruber (2004), Seasonal and long-term dynamics of the upper ocean carbon cycle at Station ALOHA near Hawaii, *Global Biogeochem. Cycles*, *18*, GB4006, doi:10.1029/2004GB002227.

Key, R. M., A. Kozyr, C. L. Sabine, K. Lee, R. Wanninkhof, J. L. Bullister, R. A. Feely, F. J. Millero, C. Mordy, and T.-H. Peng (2004), A global ocean carbon climatology: Results from Global Data Analysis Project (GLODAP), *Global Biogeochem. Cycles*, *18*, GB4031, doi:10.1029/2004GB002247.

Lefèvre, N., et al. (2004), A decrease in the sink for atmospheric CO_2 in the North Atlantic, *Geophys. Res. Lett.*, *31*, L07306, doi:10.1029/2003GL018957.

Le Quéré, C., et al. (2007), Saturation of the Southern Ocean CO_2 sink due to recent climate change, *Science*, *316*, 1735–1738, doi:10.1126/science.1136188.

Le Quéré, C., et al. (2009), Trends in the sources and sinks of carbon dioxide, *Nat. Geosci.*, *2*, 831–836, doi:10.1038/ngeo689.

Locarnini, R. A., A. V. Mishonov, J. I. Antonov, T. P. Boyer, and H. E. Garcia (2006), *World Ocean Atlas 2005*, vol. 1, *Temperature*, *NOAA Atlas NESDIS 61*, edited by S. Levitus, 182 pp., U.S. Gov. Print. Off., Washington, D. C.

Lovenduski, N., N. Gruber, and S. C. Doney (2008), Towards a mechanistic understanding of the decadal trends in the Southern Ocean carbon sink, *Global Biogeochem. Cycles*, *22*, GB3016, doi:10.1029/2007GB003139.

Madec, G., and M. Imbard (1996), A global ocean mesh to overcome the North Pole singularity, *Clim. Dyn.*, *12*, 381–388, doi:10.1007/BF00211684.

Metzl, N. (2009), Decadal increase of oceanic carbon dioxide in southern Indian surface ocean waters (1991–2007), *Deep Sea Res., Part II*, doi:10.1016/j.dsr2.2008.12.007.

Reynolds, R. W., N. A. Rayner, T. M. Smith, D. C. Stokes, and W. Wang (2002), An improved in situ and satellite SST analysis for climate, *J. Clim.*, *15*, 1609–1625, doi:10.1175/1520-0442(2002)015<1609:AIISAS>2.0.CO;2.

Sabine, C. L., et al. (2004), The oceanic sink for anthropogenic CO_2, *Science*, *305*, 367–371, doi:10.1126/science.1097403.

Schuster, U., and A. J. Watson (2007), A variable and decreasing sink for atmospheric CO_2 in the North Atlantic, *J. Geophys. Res.*, *112*, C11006, doi:10.1029/2006JC003941.

Schuster, U., A. J. Watson, N. Bates, A. Corbière, M. Gonzaalez-Davila, N. Metzl, D. Pierrot, and J. M. Santana Casiano (2009), Trends in North Atlantic sea surface pCO_2 from 1990 to 2006, *Deep Sea Res., Part II*, doi:10.1016/j.dsr2.2008.12.011.

Shea, D. J., K. E. Trenberth, and R. W. Reynolds (1992), A global monthly sea surface temperature climatology, *J. Clim.*, *5*, 987–1001, doi:10.1175/1520-0442(1992)005<0987:AGMSST>2.0.CO;2.

Sitch, S., et al. (2008), Evaluation of the terrestrial carbon cycle, future plant geography and climate-carbon cycle feedbacks using five Dynamic Global Vegetation Models (DGVMs), *Global Change Biol.*, *14*, 2015–2039, doi:10.1111/j.1365-2486.2008.01626.x.

Takahashi, T., S. C. Sutherland, R. A. Feely, and R. Wanninkhof (2006), Decadal change of the surface water pCO_2 in the North Pacific: A synthesis of 35 years of observations, *J. Geophys. Res.*, *111*, C07S05, doi:10.1029/2005JC003074.

Takahashi, T., et al. (2009a), Climatological mean and decadal changes in surface ocean pCO_2, and net sea-air CO_2 flux over the global oceans, *Deep Sea Res., Part II*, doi:10.1016/j.dsr2.2008.12.009.

Takahashi, T., S. C. Sutherland, and A. Kozyr (2009b), Global Ocean Surface Water Partial Pressure of CO_2 Database: Measurements Performed during 1968–2008 (Version 2008), *ORNL/CDIAC-152*, *NDP-088r*, Carbon Dioxide Inf. Anal. Cent., Oak Ridge Natl. Lab., U. S. Dept. of Energy, Oak Ridge, Tenn. (Available at http://cdiac.ornl.gov/oceans/LDEO Underway Database/LDEO home.html)

Thompson, D. W. J., and S. Solomon (2002), Interpretation of recent Southern Hemisphere climate change, *Science*, *296*, 895–899, doi:10.1126/science.1069270.

Wetzel, P., A. Winguth, and E. Maier-Reimer (2005), Sea-to-air CO_2 flux from 1948 to 2003: A model study, *Global Biogeochem. Cycles*, *19*, GB2005, doi:10.1029/2004GB002339.

E. T. Buitenhuis and C. Le Quéré, School of Environmental Sciences, University of East Anglia, Norwich NR4 7TJ, UK. (c.lequere@uea.ac.uk)

C. Rödenbeck, Max Planck Institut für Biogeochemie, Postfach 100164, D-07701 Jena, Germany.

S. C. Sutherland and T. Takahashi, Lamont-Doherty Earth Observatory of Columbia University, 61 Rte. 9W, PO Box 1000, Palisades, NY 10964-8000, USA.